JOURNAL OF SPACECRAFT AND ROCKETS
Vol. 41, No. 3, May–June 2004

Geostationary Orbit Transfers Using Solar Electric Propulsion with Specific Impulse Modulation

C. A. Kluever*
University of Missouri—Columbia, Columbia, Missouri 65211

Maximum-payload transfers to geostationary orbit are computed for solar-electric-propulsion spacecraft that employ specific impulse (or equivalently thrust) modulation. The optimal specific impulse profile is obtained by using a direct optimization method that is based on a calculus of variations approach. Engine models with both constant and variable efficiency are considered, and constant input power is assumed. Numerical simulations show that varying specific impulse for a Hall thruster increases the delivered payload mass when compared to transfers with a fixed specific impulse. When thruster efficiency remains constant, modulating specific impulse increases transportation rate (the payload mass advantage over a chemical-propulsion transfer divided by transfer time) by about 5–6%. However, when a more realistic variable-efficiency thruster model is applied, the transportation rate gain from thrust modulation is diminished by a factor of three. This analysis demonstrates that modulating specific impulse would offer little payload delivery gain for geostationary-orbit-raising missions using realistic Hall-thruster models.

Nomenclature

a	=	semimajor axis, km
a_T	=	thrust acceleration, m/s^2
b	=	thruster efficiency model parameter
c	=	effective jet exhaust speed, gI_{sp}, m/s
d	=	thruster efficiency model parameter, m/s
e	=	eccentricity
g	=	Earth's gravitational acceleration at sea level, m/s^2
H	=	Hamiltonian function
h, k, p, q	=	equinoctial orbital elements
I_{sp}	=	specific impulse, s
i	=	inclination, deg
J_2	=	Earth oblateness constant
M	=	5×3 matrix for powered equations of motion in the equinoctial frame
$\bar{M}$	=	3×3 matrix for powered equations of motion in the orbital frame
m	=	spacecraft mass, kg
P	=	input power, kW
r	=	orbital radius, km
T_R	=	transportation rate, kg/day
t	=	time, s
t_{SEP}	=	solar-electric-propulsion transfer time, days
$\hat{\boldsymbol{u}}$	=	unit vector in thrust direction
v	=	orbital velocity magnitude, km/s
$\boldsymbol{x}$	=	state vector of equinoctial elements $(a, h, k, p, q)^T$
$\boldsymbol{z}$	=	state vector of classical elements $(a, e, i)^T$
η	=	thruster efficiency
θ	=	true anomaly, deg
$\boldsymbol{\lambda}$	=	costate vector associated with orbital elements
$\lambda_a, \lambda_e, \lambda_i$	=	costates associated with classical orbital elements
λ_m	=	costate associated with spacecraft mass
μ	=	Earth's gravitational constant, km^3/s^2
Ω	=	longitude of the ascending node, deg
ω	=	argument of periapsis, deg

Subscripts

f	=	final value
max	=	maximum value
min	=	minimum value
0	=	initial value

Introduction

IT is well known that spacecraft propelled by solar electric propulsion (SEP) can deliver a greater payload fraction compared to vehicles propelled by conventional chemical propulsion. Previous investigations have studied the payload benefits associated with using SEP for Earth orbit transfers.[1–3] Recent papers have begun to focus on the potential payload benefits that might be realized by throttling the electric engine. Engine throttling is achieved by modulating the specific impulse I_{sp}, which in turn modulates the exhaust speed and thrust magnitude. Vadali et al.[4] present optimal Earth–Mars orbit transfers with exhaust modulation. In Ref. 4, specific impulse for a proposed plasma thruster is varied during the Earth–escape spiral, interplanetary transit, and Mars-capture spiral. Oleson[3] presents the payload advantages of using electric engines that operate with two I_{sp} settings, one single fixed I_{sp} for geostationary orbit raising and another single I_{sp} value for on-orbit stationkeeping. This analysis does not consider modulating I_{sp} during the orbit transfer. Kechichian[5] presents optimal low-thrust rendezvous maneuvers with bounded thrust modulation (or I_{sp} modulation) for relatively short-duration orbit transfers (i.e., trip time is on the order of hours). Oh et al.[6] develop analytic expressions for obtaining the optimal fixed I_{sp} value and optimal variable-I_{sp} profile for low-thrust orbit transfers. These methods are based on simplifying approximations, and the payload advantage of engine throttling is demonstrated by presenting several combined chemical-electric propulsion transfers to geostationary orbit. Despite the excellent preliminary work of the previously cited researchers, it appears that a full understanding of the payload advantages gained by I_{sp} modulation for a realistic SEP system has not yet been established.

This paper presents maximum-payload geostationary orbit transfers for SEP spacecraft with variable-I_{sp} (or engine-throttling) capability that represents a more realistic engine model than previously studied in the literature. First, the optimal steering and I_{sp} control laws are presented along with the optimization strategy for obtaining maximum-payload transfers. Next, numerical solutions for optimal orbit transfers between geostationary transfer orbit (GTO) and geostationary Earth orbit (GEO) are obtained for spacecraft both with and without I_{sp} modulation. Hall thrusters are used exclusively in

Received 2 February 2003; revision received 29 August 2003; accepted for publication 17 September 2003.

*Associate Professor, Mechanical and Aerospace Engineering Department. Associate Fellow AIAA.

this analysis. The work presented in this paper differs from the work found in Refs. 3, 5, and 6 in several ways. First, the optimal variable-I_{sp} profile is determined by using a direct optimization method based on a calculus of variations approach, which enhances the convergence properties of the numerical search. Second, this paper presents optimal solutions for long-duration, three-dimensional maneuvers. Lastly, the optimal variable-I_{sp} profile is obtained for the realistic operating scenario where thruster efficiency varies with specific impulse.

Trajectory Optimization

Equations of Motion

The Earth orbit transfer is governed by the following dynamical equations, expressed in a matrix-vector format:

$$\dot{\boldsymbol{x}} = a_T M \hat{\boldsymbol{u}} \tag{1}$$

where $\boldsymbol{x} = [a \;\; h \;\; k \;\; p \;\; q]^T$ is the state vector of equinoctial orbital elements. Definitions of the equinoctial orbital elements, as well as the individual elements of the 5×3 matrix M, are presented in detail in Ref. 7. Thrust acceleration is

$$a_T = 2\eta P / m g I_{sp} \tag{2}$$

Thruster efficiency (for Hall and ion thrusters) varies with specific impulse according to the empirical relation[3]

$$\eta = bc^2/(d^2 + c^2) \tag{3}$$

where $c = gI_{sp}$ is the effective jet exhaust speed and b and d are constants derived from thruster tests. Mass flow rate is

$$\dot{m} = -2\eta P/(gI_{sp})^2 \tag{4}$$

Because a_T is on the order of 10^{-4}, the orbit transfer will require hundreds of revolutions about the Earth, and the orbital elements will change slowly during the transfer. Therefore, orbital averaging is used to alleviate the computational burden of simulating the transfer. Averaging replaces the exact time derivatives of the equinoctial elements in Eq. (1) with the mean time derivatives. The mean rates are obtained by dividing the incremental changes in each element over a single orbit by the orbital period. The incremental element changes are obtained by integrating the powered equations over a single orbital revolution (via Gaussian quadrature) with respect to longitude angle, with all elements held fixed. Integration limits for the orbital averaging computation are set at the longitude angles for exit and entrance into the Earth's shadow (see Ref. 7 for additional details).

Problem Statement

The objective is to obtain the optimal thrust direction $\hat{\boldsymbol{u}}^*(t)$ and $I^*_{sp}(t)$ programs that maximize the final spacecraft mass (or minimizes the propellant mass) for a fixed-time transfer to GEO. The initial state for the cases considered here are elliptic orbits with energy at least equal to that of a standard GTO such that $a \geq 24{,}364$ km. The terminal state is GEO, with semimajor axis $a = 42{,}164$ km, eccentricity $e = 0$; and inclination $i = 0$ deg. No constraints on final longitude angle exist because orbital averaging removes exact angular position from the dynamical equations. Specific impulse is constrained by upper and lower bounds $I_{sp_{min}}$ and $I_{sp_{max}}$, respectively. Power is assumed to be constant in all cases considered here. Varying I_{sp} essentially modulates exhaust velocity and mass-flow rate, as indicated by Eq. (4).

Optimal Control Formulation

Optimal thrust direction $\hat{\boldsymbol{u}}^*(t)$ and $I^*_{sp}(t)$ programs are based on optimal control theory and a classical calculus of variations (COV) approach (for background information on COV theory, see Ref. 8). However, a pure COV approach is not followed here; that is, the formal two-point boundary value problem is neither formulated nor solved. The optimal control equations are derived from the Hamiltonian function, which is obtained from Eqs. (1), (2), and (4):

$$H = \boldsymbol{\lambda}^T M \hat{\boldsymbol{u}} (2\eta P / m g I_{sp}) - \lambda_m \left[2\eta P \Big/ (gI_{sp})^2 \right] \tag{5}$$

where $\boldsymbol{\lambda}$ is the vector of Lagrange multipliers, or costates, associated with the five slowly varying orbital elements. The optimality condition requires that $\partial H / \partial \hat{\boldsymbol{u}} = 0$, which leads to the optimal thrust-direction program

$$\hat{\boldsymbol{u}}^* = -M^T \boldsymbol{\lambda} / \| M^T \boldsymbol{\lambda} \| \tag{6}$$

Kechichian,[5] Sackett et al.,[9] and others have derived this optimal steering law.

Pontryagin's minimum principle[8] requires that H be minimized with respect to all admissible controls at all times. The Hamiltonian can be rewritten after substituting the respective equations for optimal thrust program [Eq. (6)] and the thruster efficiency [Eq. (3)]:

$$H = -2Pb \left[\frac{\| M^T \boldsymbol{\lambda} \| g I_{sp}}{m\left(d^2 + g^2 I^2_{sp}\right)} + \frac{\lambda_m}{d^2 + g^2 I^2_{sp}} \right] \tag{7}$$

The unconstrained optimal specific impulse is obtained by setting $\partial H / \partial I_{sp} = 0$, which yields a quadratic relation in I_{sp}. The two quadratic roots are

$$I^*_{sp} = \frac{-\lambda_m m g \pm \sqrt{\lambda_m^2 m^2 g^2 + \| M^T \boldsymbol{\lambda} \|^2 b^2 g^2 d^2}}{\| M^T \boldsymbol{\lambda} \| g^2} \tag{8}$$

Next, the Hamiltonian is computed with the two solutions from Eq. (8), and the root that minimizes H is the optimal (unconstrained) I_{sp}. For the case with constant thruster efficiency ($d = 0$), the optimal specific impulse is

$$I^*_{sp} = \frac{-2\lambda_m m}{\| M^T \boldsymbol{\lambda} \| g} \tag{9}$$

Kechichian[5] has also derived this optimal variable-I_{sp} law for an engine with constant efficiency. For the constrained control case, the optimal specific impulse is determined by Eq. (8) if $I_{sp_{min}} \leq I^*_{sp} \leq I_{sp_{max}}$. If $I^*_{sp} < I_{sp_{min}}$, then optimal specific impulse is at the lower bound, and if $I^*_{sp} > I_{sp_{max}}$ the optimal specific impulse is at the upper bound in order to minimize H.

Solution Method

As mentioned in the preceding section, the optimal control problem is not solved using a purely COV approach, which would require numerical integration of the averaged costate differential equations (e.g., the optimization code SEPSPOT[9]). Instead, a direct method is used to obtain the optimal transfer. Direct optimization methods typically exhibit a larger radius of convergence when compared to indirect methods; however, direct methods can converge to locally optimal solutions and not necessarily the global optimal solution. The optimal control problem is replaced by a nonlinear programming problem, which is solved by using a constrained parameter optimization algorithm. Sequential quadratic programming (SQP) is the parameter optimization method used here.[10] The unknown costate time histories, $\boldsymbol{\lambda}(t)$ and $\lambda_m(t)$, are parameterized by linear interpolation through a set of discrete optimization parameters (nodes) equally spaced with transfer time. Therefore, the nodal values of the costates are the SQP design variables, and the SQP algorithm adjusts these parameters so that the desired performance index (propellant mass) is directly reduced each iteration. Using the costate nodal values as the design parameters permits two distinct advantages over directly parameterizing the thrust-steering and specific impulse profiles: 1) the desirable optimal control structure from COV is enforced, and 2) the size of the SQP design space is reduced. Terminal GEO rendezvous conditions are enforced through the SQP equality constraints.

Because the final GEO target orbit only involves three constraints (a, e, and i), the three corresponding differential equations and

Table 1 Optimal GTO–GEO transfers with initial chemical stage

Case	Transfer time, days	Optimal I_{sp}, s	Thruster efficiency	Final mass, kg	Transportation rate, kg/day
1a	90	1315.2	0.5	4022	5.14
1b	90	Modulates	0.5	4045	5.39
2a	120	1940.5	0.5622	4153	4.94
2b	120	Modulates	Variable	4161	5.01

costate variables are used for the control law formulations, Eqs. (6) and (8). The differential equations for the three classical orbital elements are

$$\dot{z} = a_T \bar{M}\hat{\boldsymbol{u}} = a_T \begin{bmatrix} 0 & \dfrac{2a^2 v}{\mu} & 0 \\ \dfrac{r\sin\theta}{av} & \dfrac{2(e+\cos\theta)}{v} & 0 \\ 0 & 0 & \dfrac{r\cos(\omega+\theta)}{\sqrt{\mu a(1-e^2)}} \end{bmatrix} \hat{\boldsymbol{u}} \tag{10}$$

Matrix $\bar{M}$ in Eq. (10) is used in the thrust-direction control law (6) and I_{sp} control law (8) along with the classical element costate vector $\boldsymbol{\lambda} = [\lambda_a \;\; \lambda_e \;\; \lambda_i]^T$ and mass costate λ_m. The classical element costates are used here because they provide a more intuitive feel compared to the equinoctial element costates. For example, setting a classical costate value to an extremely large magnitude results in steering control that increases the time rate of the corresponding classical orbital element. Therefore, the nodal values of λ_a, λ_e, λ_i, and λ_m are the SQP optimization variables. Equation (1), which uses equinoctial orbital elements, is the governing dynamical equation for the orbit transfer, and the classical costates are only used to parameterize the controls. Furthermore, the thrust direction unit vector in Eq. (10) must be transformed from the velocity/orbit-plane frame to the equinoctial frame for use in Eq. (1).

Numerical Results

Several maximum-payload GTO–GEO transfers are obtained for a range of fixed transfer times. Hall thrusters are used for the orbit transfer, and thruster efficiency parameters are $b = 0.73$ and $d = 10{,}400$ m/s, respectively.[3,11] Upper and lower I_{sp} limits are 4000 and 1100 s, respectively, which represent state-of-the-art Hall thrusters according to Ref. 11. Therefore, the corresponding upper and lower thruster efficiencies are 0.682 and 0.379, respectively. Input power P is constant during the entire transfer. During the operation of certain EP devices [such as the 30-cm NASA solar electric propulsion technology applications readiness (NSTAR) ion engine], power P decreases as I_{sp} decreases.

Numerical integration of the averaged state equations is performed with a fixed-step, fourth-order Runge–Kutta routine. Integration step size is typically around 2–4 days for all transfers, and this step size is consistent with other trajectory optimization methods that use orbital averaging.[9] Earth-shadow and oblateness J_2 effects are included in the averaged dynamical equations.

Planar GTO–GEO Transfers with Initial Chemical Stage

Oh et al.[6] compared the payload advantages for planar GTO–GEO transfers with fixed- and variable-I_{sp} Hall engines, and in both cases thruster efficiency was assumed to be constant at $\eta = 0.5$. The satellite is initially launched into an equatorial GTO using Sea Launch, and the initial spacecraft mass in GTO is 5700 kg. The GTO–GEO transfer in Ref. 6 assumes that two chemical burns raise apogee and perigee such that the starting orbit for the SEP transfer is a 24-h elliptical orbit with a semimajor axis equal to 42,164 km. (The eccentricity of the starting orbit can be between zero and 0.844.) The SEP stage then utilizes an inertial-fixed steering profile in order to reduce eccentricity and circularize the orbit without changing semimajor axis. (Earth-shadow effects are ignored in Ref. 6.) Oh et al.[6] compare the performance of fixed- and variable-I_{sp} thrusters by using a metric called transportation rate, which accounts for the mass advantage associated with the SEP transfer and the corresponding transfer time. Transportation rate is

$$T_R = \Delta m / t_{\text{SEP}} \tag{11}$$

where Δm is the payload mass advantage gained from using an SEP transfer when compared to an all-chemical GTO-GEO transfer. For $m_0 = 5700$ kg, an all-chemical GTO-GEO transfer (with chemical $I_{sp} = 320$ s) delivers 3560 kg to GEO.

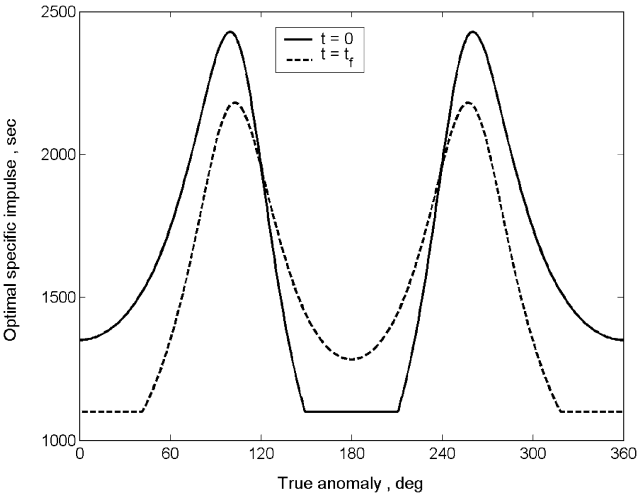

Fig. 1 Specific impulse profiles for optimal planar transfer with t_f = 90 days.

Table 1 presents optimal planar GTO-GEO transfers using the boundary conditions from Ref. 6 and the solution methods discussed in the present paper. Input power P is fixed at 9 kW, and the eccentricity of the starting orbit for the SEP transfer is 0.6. (Therefore, spacecraft mass is 4443 kg at the start of the SEP stage.) Cases 1a and 1b employ constant-efficiency thrusters; therefore, these cases can be compared to the results from Ref. 6. For a fixed-thrust/fixed-efficiency engine (case 1a), the optimal fixed specific impulse is 1315 s, and the transportation rate is 5.14 kg/day when the transfer time is fixed at 90 days. Oh et al.[6] find that with a fixed thrust-steering profile the optimal I_{sp} is 1280 s and T_R is 4.91 kg/day. Therefore, including the optimal steering profile improves transportation rate (for this case) by about 4.7% for the fixed-I_{sp} thruster. Table 1 shows that modulating specific impulse during the transfer (case 1b) improves transportation rate by about 4.9% when compared to the fixed-I_{sp} transfer (case 1a). Oh et al.[6] show that transportation rate in increased by about 10% when specific impulse is modulated. Our results show that including the optimal thrust steering profile narrows the performance gap between the fixed- and variable-I_{sp} transfers. Figure 1 presents the optimal specific impulse profile during the initial and final orbital revolutions for case 1b. (Earth-shadow eclipses are not shown in Fig. 1 in order to clearly present the optimal I_{sp} profile over a single revolution.) Note that engine thrust is maximized (caused by minimum I_{sp}) near apogee during the initial revolutions and at perigee during the final revolutions. Engine throttle is reduced when true anomaly is near ± 90 deg because thrust has a diminished effect on the dynamical equation for eccentricity.

Cases 2a and 2b are optimal transfers with variable thruster efficiency governed by Eq. (3). It was not possible to obtain 90-day transfers with the variable-efficiency model because the thrust magnitude was too small as a result of the low I_{sp} and degraded thruster efficiency. Therefore, the trip time for cases 2a and 2b is fixed at 120 days. Note that modulating specific impulse improves transportation rate over the fixed-throttle case, but the T_R increase is only 1.4%. Reference 6 does not present GTO–GEO solutions with variable thruster efficiency.

Maximum-Payload, Three-Dimensional GTO–GEO Transfers

The starting orbit for the SEP transfer is GTO, with $a = 24,364$ km; $e = 0.7306$; $i = 28.5$ deg, and $\Omega = \omega = 0$ deg. The initial spacecraft mass is 1790 kg, which represents the GTO launch capability of the Delta 7925 booster. Earth-shadow effects are included, and input power P is fixed at 10 kW.

A single representative optimal GTO–GEO transfer is discussed before analyzing the family of solutions. Transfer time is fixed at 80 days for the representative case, and thruster efficiency varies according to Eq. (3). Figures 2 and 3 present the optimal pitch and yaw thrust steering angles for a maximum-payload transfer with variable specific impulse. Pitch angle is measured in the orbital plane from the velocity vector to the projection of the thrust vector, and yaw angle is measured from the orbit plane to the thrust vector. Figures 2 and 3 show pitch and yaw steering profiles during a complete orbital revolution for the beginning, middle, and end of the GTO–GEO transfer. (Earth-shadow periods, where thrust is zero, are not shown in these figures in order to preserve clarity of the steering program.) Note that pitch steering angle is initially small (nearly tangent steering) for maximum energy gain and that the pitch angle amplitude increases in order to reduce eccentricity. The terminal pitch steering profile is close to an inertial-fixed steering program and concentrates on circularizing the orbit. Figure 3 shows that the out-of-plane steering angle is initially large at the nodal crossing at apogee ($\theta = 180$ deg) in order to reduce inclination. Yaw steering is slightly asymmetric about apogee during the middle part of the transfer because the apse line is slightly rotated (ω is around 20 deg) because of Earth oblateness and unbalanced thrust caused by Earth-shadow effects. Figures 4 and 5 summarize the maximum, minimum, and average I_{sp} and thrust values over the entire transfer. Figure 4 shows that optimal I_{sp} is near the lower bound at the beginning of the transfer in order to produce relatively large thrust (Fig. 5) and that modulation is narrow. Modulation range increases with trip time, and specific impulse is smallest at perigee and apogee (apsidal crossings) during the early and later stages of the transfer. Specific impulse (and thrust) experience the greatest modulation near the middle portion of the orbit transfer.

Next, a family of maximum-payload solutions is presented. Figure 6 presents the maximum payload solutions for a Hall thruster with fixed efficiency ($\eta = 0.5$) and variable efficiency [Eq. (3)], as

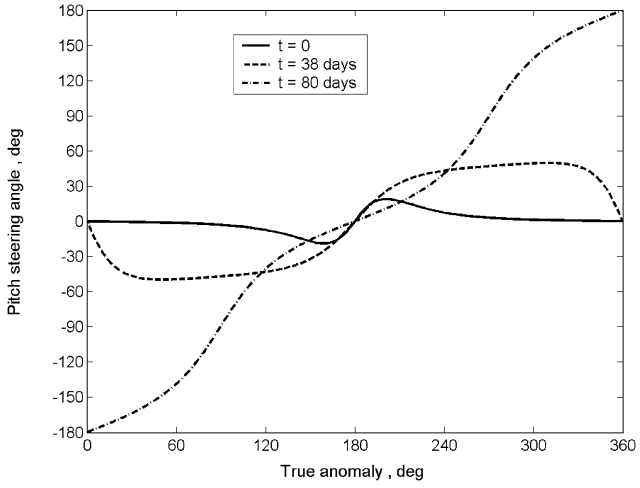

Fig. 2 Pitch steering angle profiles for optimal three-dimensional GTO–GEO transfer with t_f = 80 days.

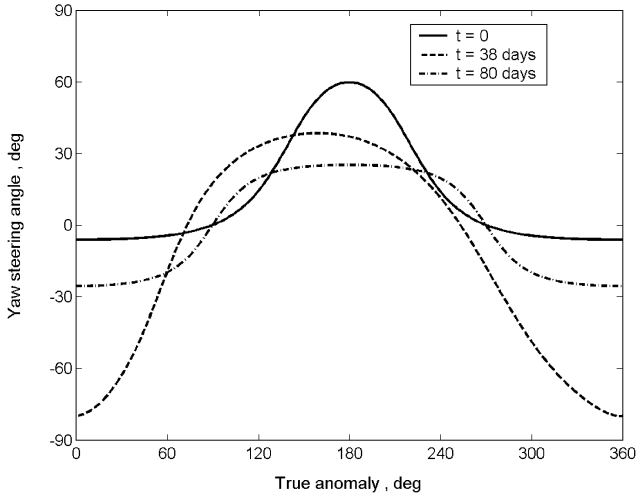

Fig. 3 Yaw steering angle profiles for optimal three-dimensional GTO–GEO transfer with t_f = 80 days.

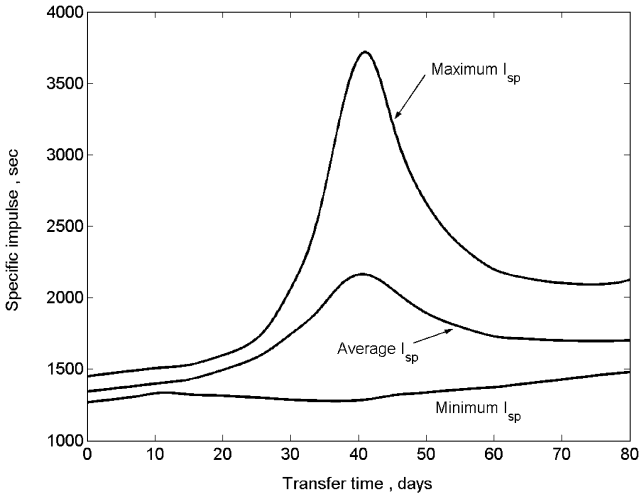

Fig. 4 Specific impulse amplitude vs transfer time for three-dimensional GTO–GEO transfer.

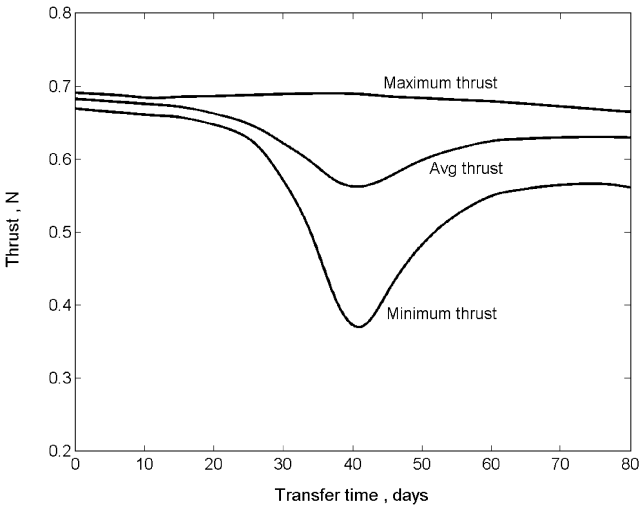

Fig. 5 Thrust amplitude vs transfer time for three-dimensional GTO–GEO transfer.

Next, a family of maximum-payload solutions is presented. Figure 6 presents the maximum payload solutions for a Hall thruster with fixed efficiency ($\eta = 0.5$) and variable efficiency [Eq. (3)], as

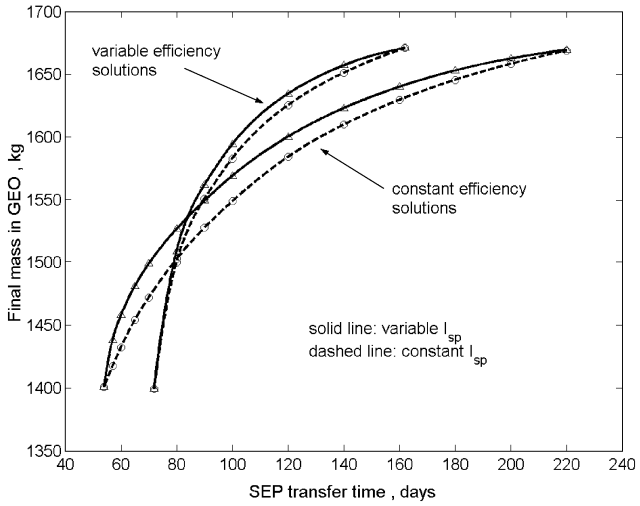

Fig. 6 Maximum payload solutions vs fixed transfer time.

well as operation with a single (constant) optimal I_{sp} and an optimal variable-I_{sp} profile governed by Eq. (8). Each symbol represents an optimal solution. Figure 6 clearly shows that the final delivered mass to GEO increases as fixed SEP transfer time increases and that throttling the engine slightly improves the final mass when compared to a transfer with a fixed I_{sp}. The maximum gain in payload mass caused by engine throttling is about 26.9 kg (for $t_{SEP} = 65$ days) for the fixed-efficiency thruster, and the maximum payload gain is about 11.3 kg (for $t_{SEP} = 85$ days) for the variable-efficiency thruster. Both sets of curves show that the constant- and variable-efficiency engines produce the same minimum (1400 kg) and maximum (1670 kg) values for final mass. The respective minimum transfer times (53 and 72 days) correspond to minimum-time transfers with specific impulse fixed at the lower bound $I_{sp} = 1100$ s (maximum thrust). Similarly, the respective maximum transfer times (160 and 220 days) correspond to maximum-payload transfers with free end time and $I_{sp} = 4000$ s. The constant- and variable-I_{sp} solutions converge at these upper and lower time-of-flight limits. Therefore, engine throttling provides very little mass benefit when the SEP transfer time is either near the minimal value or exceptionally long.

Figures 7a and 7b present the transportation rate for the trials with a constant- and variable-efficiency Hall thruster. The fixed-efficiency engine (Fig. 7a) shows a wider range in transportation rate (8 to 3 kg/day) compared to the variable-efficiency engine (Fig. 7b; T_R ranges from 6.5 to 4 kg/day). The maximum increases in T_R as a result of modulating specific impulse are about 0.5 and 0.2 kg/day for the fixed- and variable-efficiency engines, respectively. As the gain in payload mass "flattens" with increased transfer time (see Fig. 6), the transportation rate steadily decreases as seen in Figs. 7a and 7b.

The fixed-efficiency solutions presented in Fig. 7a are consistent with the results presented by Oh et al.[6] Figure 8 presents the improvement in T_R caused by specific impulse modulation for the general three-dimensional GTO–GEO transfer considered in this paper, and the maximum improvement in T_R is about 6% for the fixed-efficiency engine. When thruster efficiency varies with specific impulse according to Eq. (3), the transportation rate advantages from throttling the engine are diminished, as seen by the lower curve in Fig. 8. Maximum increase in transportation rate from throttling the engine is only about 2% when transfer time is around 85 days. A 2% increase in T_R for a transfer time of 85 days is equivalent to increasing the payload fraction (m_f/m_0) from 0.8663 (fixed throttle) to 0.8726 (with throttling). Both sets of solutions show that any increase in transportation rate from throttling the engine diminishes as transfer time increases. Furthermore, engine throttling is not possible when the transfer time is at the minimum-time value because maximum thrust (i.e., minimum I_{sp}) is necessary to complete the transfer.

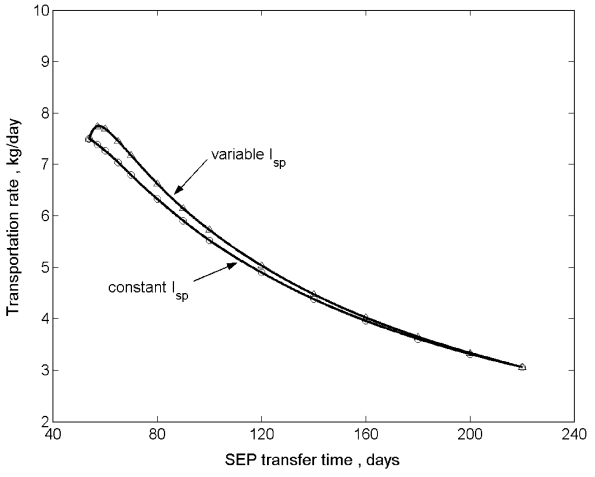

a)

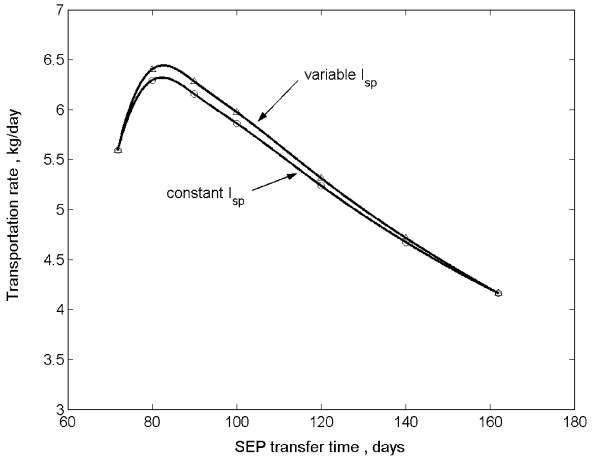

b)

Fig. 7 Transportation rate vs fixed transfer time: a) fixed-efficiency thruster and b) variable-efficiency thruster.

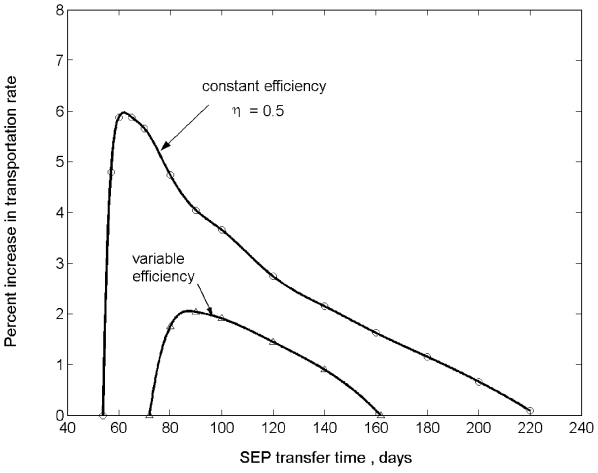

Fig. 8 Percent improvement in transportation rate as a result of specific impulse modulation.

Conclusions

Optimal orbit transfers using electric propulsion with specific impulse modulation have been obtained. A numerical approach for determining the optimal specific impulse profile for engines with variable efficiency has been developed and tested. The solution technique is based on the optimal control laws for thrust direction and specific impulse modulation that are derived by using a calculus of variations approach. A direct parameter optimization method is

used to select the optimal costate profiles that produce the optimum thrust steering and I_{sp} profiles. The direct method provides a robust solution technique, and optimal trajectories are readily obtained for long-duration transfers that include Earth-shadow effects.

Several maximum-payload GTO–GEO transfers are obtained for a wide range of transfer times. Solutions are determined for Hall thrusters with fixed- and variable-propulsion efficiency. Results show that throttling a fixed-efficiency thruster increases the transportation rate by about 5–6% at best when compared to a fixed-I_{sp} engine. These results are consistent with previous analyses in the literature that only considered fixed-efficiency thrusters. However, the payload gains are significantly diminished when the more realistic variable-efficiency engine model is employed. Throttling a variable-efficiency Hall thruster increases the transportation rate by about 2% at best when compared to a fixed-I_{sp} engine. In addition, the variable-efficiency engine increases the SEP transfer time that provides the maximum transportation rate advantage by about 20 days (or 31%). The additional electronic hardware necessary to implement variable-I_{sp} operation can exceed the slight mass advantage gained by engine throttling. Based on these analyses with realistic Hall engine models, it appears that modulating specific impulse would offer little payload delivery gain for geostationary-orbit-raising missions using Hall thrusters. However, using thrusters with different efficiency curves (such arcjet and plasma thrusters) or different orbit transfer scenarios can result in a larger benefit from modulating specific impulse.

References

[1]Spitzer, A., "Near Optimal Transfer Orbit Trajectory Using Electric Propulsion," American Astronautical Society, AAS Paper 95-215, Feb. 1995.

[2]Oleson, S. R., and Myers, R. M., "Advanced Propulsion for Geostationary Orbit Insertion and North–South Station Keeping," AIAA Paper 95-2513, July 1995.

[3]Oleson, S. R., "Mission Advantages of Constant Power, Variable I_{sp} Electrostatic Thrusters," AIAA Paper 2000-3413, July 2000.

[4]Vadali, S. R., Nah, R., Braden, E., and Johnson, I. L., "Fuel-Optimal Planar Earth-Mars Trajectories Using Low-Thrust Exhaust-Modulated Propulsion," *Journal of Guidance, Control, and Dynamics*, Vol. 23, No. 3, 2000, pp. 476–482.

[5]Kechichian, J. A., "Optimal Low-Thrust Transfer Using Variable Bounded Thrust," International Astronautical Federation, Paper 93A.2.10, Oct., 1993.

[6]Oh, D. Y., Randolph, T. R., Snyder, J. S., Martinez-Sanchez, M., and Kimbrel, S., "Optimum Specific Impulse Profiles for Mixed Chemical-Electric Orbit Raising Missions," *Proceedings of the 2nd Low-Thrust (LOTUS2) International Symposium*, edited by J. Fourcade and S. Geffroy, Centre National d'Etudes Spatials, Toulouse, France, 2002.

[7]Kluever, C. A., and Oleson, S. R., "Direct Approach for Computing Near-Optimal Low-Thrust Earth-Orbit Transfers," *Journal of Spacecraft and Rockets*, Vol. 35, No. 4, 1998, pp. 509–515.

[8]Bryson, A. E., and Ho, Y.-C., *Applied Optimal Control*, 1st ed., Hemisphere, New York, 1975, pp. 47–110.

[9]Sackett, L. L., Malchow, H. L., and Edelbaum, T. N., "Solar Electric Geocentric Transfer with Attitude Constraints: Analysis," NASA CR-134927, Aug. 1975.

[10]Pouliot, M. R., "CONOPT2: A Rapidly Convergent Constrained Trajectory Optimization Program for TRAJEX," Convair Div., General Dynamics, GDC-SP-82-008, San Diego, CA, Jan. 1982.

[11]Butler, G. W., Yuen, J. L., Tverdokhlebov, S. O., Semenkin, A. V., and Jankovsky, R. S., "Multi-Mode, High Specific Impulse Hall Thruster Technology," AIAA Paper 2000-3254, July 2000.

C. McLaughlin
Associate Editor